Published in final edited form as:
J Comp Neurol. 2010 June 1; 518(11): 2035–2050. doi:10.1002/cne.22320.

Synaptic Input of ON-Bipolar Cells onto the Dopaminergic Neurons of the Mouse Retina

Massimo Contini[1], **Bin Lin**[2], **Kazuto Kobayashi**[3], **Hideyuki Okano**[4], **Richard H. Masland**[2], and **Elio Raviola**[1]

[1] Department of Neurobiology, Harvard Medical School, Boston, Massachusetts 02115

[2] Massachusetts Eye and Ear Infirmary, Harvard Medical School, Boston, Massachusetts 02114

[3] Department of Molecular Genetics, Fukushima Medical University School of Medicine, Hikarigaoka, Fukushima 960-1295, Japan

[4] Department of Physiology, Keio University School of Medicine, 35 Shinanomachi, Shinjuku-ku, Tokyo 160-8582, Japan

Abstract

In the retina, dopamine fulfills a crucial role in neural adaptation to photopic illumination, but the pathway that carries cone signals to the dopaminergic amacrine (DA) cells was not known. We identified the site of ON-cone bipolar input onto DA cells in transgenic mice in which both types of catecholaminergic amacrine (CA) cells were labeled with green fluorescent protein or human placental alkaline phosphatase (PLAP). In confocal Z series of retinal whole mounts stained with antibodies to tyrosine hydroxylase (TH), DA cells gave rise to varicose processes that descended obliquely through the scleral half of the inner plexiform layer (IPL) and formed a loose, tangential plexus in the middle of this layer. Comparison with the distribution of the dendrites of type 2 CA cells and examination of neurobiotin-injected DA cells proved that their vitreal processes were situated in stratum S3 of the IPL. Electron microscope demonstration of PLAP activity showed that bipolar cell endings in S3 established ribbon synapses onto a postsynaptic dyad in which one or both processes were labeled by a precipitate of lead phosphate and therefore belonged to DA cells. In places, the postsynaptic DA cell processes returned a reciprocal synapse onto the bipolar endings. Confocal images of sections stained with antibodies to TH, kinesin Kif3a, which labels synaptic ribbons, and glutamate or $GABA_A$ receptors, confirmed that ribbon-containing endings made glutamatergic synapses onto DA cells processes in S3 and received from them GABAergic synapses. The presynaptic ON-bipolar cells most likely belonged to the CB3 (type 5) variety.

Keywords

transgenic mice; immunocytochemistry; electron microscopy; GFP; PLAP; amacrine cells

Introduction

Dopamine is the catecholamine modulator responsible for changes in the gain of retinal synapses, a shift that occurs during neural adaptation to light (see Witkovsky and Dearry 1991; Djamgoz and Wagner 1992). It is synthesized and released in a paracrine fashion (Puopolo et al. 2001) by the dopaminergic amacrine (DA) or type 1 catecholaminergic cells,

Correspondence: Elio Raviola , Department of Neurobiology, Harvard Medical School, 220 Longwood Avenue, Boston, MA 02115 **Tel.** 617 432 1742 **Fax:** 617 734 7557 elio_raviola@hms.harvard.edu.

diffuses throughout the intercellular spaces of the retina and acts by volume transmission (Witkovsky et al. 1993; Bjelke et al. 1996) on most types of retinal neurons, setting the gain of retinal networks for cone-mediated (photopic) vision (Witkovsky 2004). Dopamine is released upon illumination of the retina and flickering light is a better stimulus than a steady background luminosity; there is, however, a basal release in the dark and, in addition, DA cells contain a circadian clock that influences dopamine synthesis and release, anticipating predictable variations in retinal illumination (Kramer 1971; Boatright et al. 1989; Dorenbos et al. 2007; see also Witkovsky and Dearry 1991, Djamgoz and Wagner 1992, Witkovsky et al. 2003, Witkovsky 2004). Recordings from DA cell have indeed confirmed recently that light excites a proportion of these neurons and causes a transient increase in the frequency of their discharge of action potentials (Zhang et al. 2007, 2008).

Because of the effect of photopic light on dopamine release, one would expect that DA cells receive excitatory synaptic input from depolarizing or ON-cone bipolar cells, whose axonal arborizations are situated in the *b* or ON- sublamina of the inner plexiform layer (IPL). It is well known that the axonal arborizations of bipolar cells and their synaptic targets, the dendrites of ganglion cells, are rigorously stratified in the IPL: of the five layers or strata originally described by Cajal (1893), the two more scleral strata (S1 and S2) are the site of the synapses between OFF- cone bipolars and OFF-ganglion cells and together comprise the *a* or OFF-sublamina of the IPL. The remaining three, more vitreal strata (S3, S4, S5) comprise the *b* sublamina and contain the synapses between ON- cone bipolars and ON-ganglion cells (S3, S4, S5) as well as those established by rod bipolars with two classes of rod amacrine cells that are located in S5 (Famiglietti and Kolb 1976, cat; Nelson et al. 1978, cat; Euler et al. 1996, rat; McGillem and Dacheux 2001, rabbit; Ghosh et al. 2004, mouse). In contrast with this expectation, previous electron microscopic studies reported the presence of synapses between bipolar endings and DA cell processes in S1, rather than deeper in the IPL. Since all bipolar cell synapses are glutamatergic and excitatory, one could argue that in S1 DA cells would receive input from OFF-bipolars that release transmitter upon dimming of the light. There is no agreement, however, on the frequency of these synapses in retinas of different species. No bipolar synapses onto DA cells are described in early studies of rabbit, cat and primate retinas (Dowling and Ehinger 1975, 1978; Dowling et al. 1980; Frederick et al. 1982; Pourcho ’82). According to Hokoç and Mariani (1987, 1988), bipolar synapses in the S1 stratum represented 53% of the total synaptic input onto DA cell processes in the rhesus macaque, 26% in the cat and 62% in the rabbit, but the density of the synapses was not stated. Postsynaptic dyads were present in all three species; in the rabbit, monads were found as well. According to Kolb et al. (1990), in the S1 stratum of the cat the bipolar synapses onto DA cells were very rare, whereas in the mouse, Gustincich et al. (1997) reported the presence of monads.

Because of the apparent discrepancy between the physiological and anatomical findings, we decided to re-examine the issue of the bipolar input onto DA cells. In fact, there are other potential candidates in the anatomy of these neurons as the site of the ON-bipolar input. The DA cells’ perikarya, situated in the inner nuclear layer, give rise to both dendrites and axons (Dacey 1988,1990;Witkovsky et al. 2005) that run tangentially in the retina, forming a dense plexus in the stratum S1 of the IPL. In a few species, such as the rabbit, DA cells are typical amacrines, i.e., their processes do not extend sclerally beyond the IPL (Tauchi et al. 1990). In most other species, they are interplexiform cells, because they send additional processes to the outer plexiform layer (OPL), where they form a second plexus, whose richness varies greatly among different animals (see Nguyen-Legros 1988). Importantly for this study, DA cells appear to possess a small number of additional processes that descend vitread from the main plexus in S1 and form a third, loose plexus in the middle of the IPL (Nguyen-Legros et al. 1981, rat, M. fascicularis; Brecha et al. 1984, rabbit; Hokoç and Mariani 1987,1988, cat, rabbit, M. mulatta; Wulle and Schnitzer 1989, mouse; Tauchi et al. 1990 rabbit; Casini and

Brecha 1992, rabbit; Zang et al. 2007,suppl. Fig. 4). Finally, in some species, DA cell processes appear to give rise to a fourth plexus in the deepest region of the IPL (Nguyen-Legros et al. 1981,1982, rat, M. fascicularis; Hokoç and Mariani 1987,1988 cat, rabbit; Dacey 1990, M. mulatta; Kolb et al. 1990, cat; Tauchi et al. 1990, rabbit; Wang et al. 1990, cat), where they synapse with the dendrites of AII amacrines (Kolb et al. 1990). Occasionally, the deep processes of DA cells, after a tangential course of several hundred micrometers, ascend back to S1.

DA cell processes in S3 could be the recipients of the ON-cone bipolar synapses, but there is a confounding circumstance that complicates the interpretation of the observations quoted above: Most of the descriptions of DA cells are based on immunocytochemical demonstration of tyrosine hydroxylase (TH), the rate limiting enzyme in dopamine biosynthesis, and the retina contains a second type of TH-positive neuron, the type 2 catecholaminergic amacrine (CA) cell, whose single dendrite gives rise to an arbor residing in the S3 stratum (Mariani and Hokoç 1988, M. mulatta; Wang et al. 1990, cat). This type of neuron, however, exhibits a smaller perikaryon than DA cells and is less intensely stained by antibodies to TH.

In this paper, we report the results of a study on the synaptic connections of the S3 processes of DA cells in the mouse, a species in which there is no DA cell plexus in S5. To this purpose, we used two transgenic lines, one in which catecholaminergic neurons are labeled with green fluorescent protein (GFP) and the other in which they are labeled with human placental alkaline phosphatase (PLAP). In these lines, type 2 CA cells are not stained by antibodies to TH, thus eliminating any ambiguity as to the origin of the S3 processes in retinas stained for TH immunocytochemistry.

Materials and Methods

Animals

We used wild type C57BL/6J mice (Jackson Laboratory, Bar Harbor, ME); transgenic C57BL/6J × DBA/2J hybrids, expressing GFP under control of the 9.0 kb 5′-flanking region of rat TH gene (Matsushita et al. 2002); transgenic C57BL/6J mice expressing PLAP under control of a 4.8 kb promoter sequence of the rat TH gene (Gustincich et al. 1997). All procedures involving mice were in accordance with National Institutes of Health guidelines and approved by the Institutional Animal Care and Use Committee of Harvard Medical School.

Immunocytochemistry

The wild type and GFP mice were anesthetized by IP injection of a 0.1 ml solution containing equal parts of 5% ketamine (Ketaset; Bristol-Myers Co., Syracuse, NY) and 1% xylazine (Rompun; Bayer Co., Shawnee Mission, KS). Either their vascular system was perfused through the heart with carbo-oxygenated Ames medium (Sigma-Aldrich Inc., St Louis, MO) containing 40 mM glucose, 0.1% procaine and 0.001% heparin, followed by 2% formaldehyde in 0.15 M Sörenson phosphate buffer (pH 7.4) or the eyes were enucleated, opened at the equator and immersed in the same fixative fluid. Retinas were separated from the pigment epithelium and remaining ocular tunics and kept in the fixative fluid for additional 2hr at room temperature.

For immunostaining with the antibodies to $GABA_A$ receptors subunits (a gift from W. Sieghart, University of Vienna, Vienna), whose epitopes were very sensitive to denaturation by fixatives, mice were given a lethal dose of sodium pentobarbital and their eyes were enucleated; posterior eyecups were immersed in Ames medium and retinas were separated from the other ocular tunics. The specimens were immersed in 3 ml 2% formaldehyde in

Sörenson phosphate buffer in 30mm Petri dishes, fixed for 15-17 s in a microwave oven (Pelco; Ted Pella, Inc., Redding, CA) and rapidly transferred to phosphate buffered saline (PBS). Upon irradiation, the final temperature of the fixative increased to 55-60°C.

To investigate the distribution of the TH-positive processes of DA cells in whole mounts, retinas of the GFP mice were washed in PBS; preincubated for 2hr to overnight in blocking solution containing 2% bovine serum albumin (BSA, Sigma-Aldrich), 10% normal goat serum (Cat#S-1000, Vector Labs, Burlingame, CA), 2% fish gelatin (Goldmark Biologicals, Phillipsburg, NJ), 0.05% Triton X-100, 0.1% sodium azide in PBS; incubated in a mixture of monoclonal and sheep polyclonal α-TH antibodies (see below) for 3 days at room temperature; washed several hours in block solution, followed by a 3 day incubation in a mixture of α-mouse and α-sheep secondary donkey antibodies both conjugated to Alexafluor 568 (1:500; Cat# A10037 and A21099 resp., Invitrogen-Molecular Probes, Carlsbad, CA). The antibodies were diluted with 2% BSA. The retinas were finally rinsed in several changes of PBS and mounted in Vectashield (Vector Labs).

To identify the bipolar synapses by confocal microscopy, we triple-stained radial and tangential sections of the retina with the sheep polyclonal α-TH, a mouse monoclonal α-kinesin II, and one of the following rabbit polyclonal antibodies: α-glutamate receptor 1, α-glutamate receptor 2/3, α-α1 and α-β1 subunits of the $GABA_A$ receptor (see below). To this purpose, fixed retinas were washed in PBS, cryoprotected in 20% sucrose in PBS, frozen in the liquid phase of partially solidified monochlorodifluoromethane and finally cut in a cryostat at a thickness of 5-10 μm. The rest of the procedure followed the protocol described above, but Triton X-100 and sodium azide were omitted and the incubation times were reduced to 3 – 12 hr.

Secondary antibodies were: Alexafluor 568 goat α -mouse (Cat# A-11031, Invitrogen-Molecular Probes); Alexafluor 568 goat α -rabbit (Cat#A-1103, Invitrogen-Molecular Probes); Alexafluor 660 donkey α -sheep (Cat #A-21101, Invitrogen-Molecular Probes); Alexa Fluor 488 goat α -rabbit (Cat. #A-11008, Invitrogen-Molecular Probes); Alexafluor 488 goat α-mouse (Cat#A-11001, Invitrogen-Molecular Probes). All secondary antibodies were used at the dilution of 1:500.

Ethidium bromide (Cat #15585-011, Invitrogen-Molecular Probes) in PBS was applied to some sections to counterstain nuclei.

Antibody Characterization

See Table 1 for a list of all antibodies used. With the exception of the two α-$GABA_A$ receptor antibodies, the reagents listed in the table showed a distribution within the retina that was identical to that described for their epitopes in a large number of previous reports concerning both the mouse and other mammalian species.

1. The α-TH monoclonal, after SDS-PAGE and Western blotting, recognized the expected single band of 60 kD in cell extracts of HEK293 cells transiently transfected with cDNA of human TH isoform 2. In our hands, this monoclonal stained exclusively the expected types of dopaminergic neurons in sections of both retina and midbrain. Furthermore, the staining of DA cells with this antibody coincided with that of the sheep polyclonal described below.
2. The α-TH sheep polyclonal recognized the expected single band of about 60 kD in a PC12 cell lysate. We have extensively used this antibody and consistently observed that it co-localized in the retina and midbrain with the monoclonal described above.

3. The K2.4 antibody detects the 85 kD component of sea urchin kinesin II. It cross-reacts with a protein doublet corresponding to Kif3a in Western blots of rat brain extract and typically stained the horseshoe-shaped synaptic ribbons of vertebrate photoreceptors (Muresan et al. 1999) and the punctate ribbons of axonal endings of bipolar cells (Jakobs et al. 2008).

4. Western blot analysis of rat brain showed that the affinity-purified α-glutamate receptor 1 (GluR1) antibody recognized a single band co-migrating with GluR1 expressed in transfected cells. In our hands, the antibody stained spots in the OPL and IPL that coincided with kinesin II-stained synaptic ribbons. It therefore labeled the expected sites of the postsynaptic AMPA receptor clusters of glutamatergic synapses established by cone photoreceptors with OFF-cone bipolars in the OPL and by bipolar cell axons with ganglion cell dendrites in the IPL.

5. According to the manufacturer, Western blot analysis of rat brain showed that the affinity-purified α-glutamate receptor 2/3 (GluR2/3) antibody recognized two bands that co-migrated with GluR2 and GluR3 expressed in transfected cells. In our hands, the antibody showed the same localization as the antibody to GluR 1 described above.

6. The affinity purified antibody to the $GABA_A$ receptor ⟨1 subunit recognized in Western blots a single 51 kD band that co-migrated with affinity-purified $GABA_A$ receptor from rat brain (Zezula and Sieghart 1991a). It also selectively recognized a 51 kD protein photolabeled by $^{[3]}$flunitrazepam (Zezula et al. 1991b). The distribution of this antibody in the brain was extensively characterized by immunocytochemistry (Zimprich et al. 1991, Nusser et al 1995; Sperk et al. 1997). The presence in DA cells of the transcript for the ⟨1 subunit was established by single-cell RT-PCR and staining with this antibody confirmed that clusters of ⟨1 subunits were expressed at the cell surface (Gustincich et al 1999).

7. The antibody to the β1 subunit of the $GABA_A$ receptor was raised in the rabbit against a fusion protein transcribed in *E. coli* from a DNA construct that comprised the maltose-binding protein gene and a sequence from the receptor subunit gene. Data on the characterization of this antibody are not available. However, the presence of the transcript for the β1 subunit gene was established in DA cells by single-cell RT-PCR (Gustincich et al 1999). Furthermore, this antibody stained GABAergic synapses at the surface of DA cells because it was associated with the α3 subunit in 15% of the 261 subunit clusters examined. (Gustincich et al 1999). In this paper we combined the antibodies to both the ⟨1 and β1 subunits to enhance the staining of the receptor clusters.

All antibodies were tested on vertical sections of mouse retina before use in co-localization studies. It should be noted that the topographic coincidence of three antibody stains at the site of a single DA cell synapse and the co-localization at the coincidence sites of multiple receptor subunits, represent a powerful confirmation of the reagents' specificity.

Confocal Microscopy

For single images of retinal sections and Z series of retinal whole mounts, fluorescence was detected in a Zeiss LSM 510 Meta confocal imaging system (Carl Zeiss MicroImaging Inc., Thornwood, NY) equipped with three visible wavelength lasers, META spectral emission detectors and a Zeiss Axioplan 2 microscope. We used a 40X EC Plan-Neofluar objective 1.4 NA. After adopting the minimal thickness of the optical section that was compatible with adequate emission, images were obtained sequentially from two or three channels by averaging 8 scans (1024 × 1024 pixels) and stored as TIFF files. Brightness and contrast were adjusted by Adobe Photoshop (Adobe Systems, Mountain View, CA).

Neurobiotin Injections

GFP mice were given a lethal dose of sodium pentobarbital and the eyes were enucleated. Posterior eyecups were immersed in Ames medium and retinas were isolated. Under visual control, DA cells were penetrated with pipettes whose resistance was ~150 MΩ. The electrode tips were filled with 4% neurobiotin (Vector Labs.) and 0.5% Lucifer Yellow-CH (Invitrogen-Molecular Probes) in 0.1M Tris/HCl buffer pH 7.6 or distilled water and back-filled with 3M lithium chloride. Neurobiotin was iontophoresed with biphasic (+1.0 nA for 100 ms and −1.0 nA for 100 ms at 3 Hz for 1-2min) or monophasic (+1 nA, 3 Hz for 1-4 min) current. After the last injection, retinas were immersed in 4% formaldehyde in Sörenson phosphate buffer for 15-30 min, washed in PBS containing 0.05% Triton X-100, 1% sodium azide and reacted overnight at room temperature with Alexa 594-streptavidin conjugate (1:100; Cat#S32356, Invitrogen-Molecular Probes) in Triton-sodium azide PBS. The retinas were finally rinsed in several changes of PBS and mounted in Vectashield (Vector Labs).

To obtain single images of these wide-spreading cells, montages of neurobiotin-injected DA cells were captured by using the same confocal imaging system specified above. Z series were obtained wherever the processes weaved in and out of the optical section. Images were printed in a Laserjet 4.000N (Hewlett Packard, Palo Alto, CA) and pasted together, thus collapsing the entire cell into its orthogonal projection. The cell was then accurately traced by India ink on 54 cm-wide vellum paper rolls, photographed with a professional digital camera and stored as TIFF file.

Light and Electron Microscopic Demonstration of PLAP Activity

For demonstration of PLAP activity at the light and electron microscopes, details of the technique of specimen preparation were described previously (Gustincich et al. 1997). Briefly, anesthetized adult mice, homozygous for PLAP cDNA, were perfused through the heart with 2% formaldehyde and 1% glutaraldehyde in Sörenson phosphate buffer after rinsing the vascular tree with Ames medium as specified above. Whole retinas were kept in the fixative fluid for 2 hr at room temperature, heated in PBS at 65°C for 30 min and carefully rinsed with 5% sucrose in 0.2 M cacodylate buffer pH 7.4 to eliminate phosphate ions. Specimens were then incubated for 8-48 hr at room temperature under constant, mild agitation in a β-glycerophosphate, alkaline lead citrate solution, according to Mayahara et al. (1967). They were subsequently postfixed in 3% glutaraldehyde, followed by osmium-ferrocyanide, staining *en bloc* with uranyl acetate, dehydration and embedding in an Epon-Araldite mixture. For light microscopy, thick (1 μm) sections were treated with 1% ammonium sulfide for 5 min over a hot plate and photographed under DIC illumination with a NIKON Eclipse E600 microscope. After thin sectioning, electron micrographs were obtained with a JEOL 1200EX microscope.

Results

S3 Processes of DA Cells

Retinas of GFP mice were simultaneously stained witha monoclonal and a polyclonal antibody to TH, followed by two secondary antibodies both conjugated to the same fluorophore. With this stratagem, the beaded appearance of the finest processes of DA cells disappeared and they could be traced for long distances in their tangential course within the plexiform layers. Examination of retina whole mounts with the confocal microscope showed that both DA and type 2 CA cells expressed GFP, although to a different extent, with type 2 CA cells more intensely fluorescent than DA cells.

This finding was in striking contrast with the result of TH immunocytochemistry, where DA cells were intensely stained by TH antibodies and type 2 CA cells were completely negative (Fig. 1 A-C). Because of this fortunate circumstance, we could rule out any uncertainty as to the parent neuron of the processes of the two cell types when co-stratified within the S3 of the IPL.

Confocal Z series confirmed that the TH-positive processes emanating from the large (15 μm diameter) perikaryon of DA cells, comprised a dense plexus in the most scleral stratum of the IPL (Fig. 2A), typically perforated by circular openings occupied by the perikarya of AII amacrine cells (Törk and Stone 1979,Voigt and Wässle 1987). This S1 plexus gave rise to a small number of processes that traversed the inner nuclear layer in an oblique direction, angled at the vitreal boundary of the OPL and finally acquired a tangential course in the middle of this layer, just beneath the array of photoreceptor endings (not shown).

On the other hand, from the vitreal surface of the S1 plexus originated another set of TH positive processes, relatively few in number, that descended obliquely through the scleral half of the IPL and finally ran a long, straight, tangential course in the middle of this layer (Fig. 2B). They crossed each other at various angles and occasionally branched, thus forming a loose plexus that demarcated wide, irregular meshes. Their thickness (0.5 to 1 μm) was relatively uniform, except for the presence of varicosities, up to 2 μm in diameter, which occurred at irregular intervals along their length. The density of the varicosities was 1,500-2,000/μm^2. Examination of the GFP fluorescence showed that the intensely stained, type 2 CA cells possessed small (11μm in diameter), pyriform perikarya that gave rise to a single apical dendrite (Fig. 1C). The dendrite descended vertically to the middle of the IPL and resolved into a dense plexus (Fig. 1C and 2C), rigorously confined to the center of the S3 stratum (Fig. 1C, inset). The vitreal plexus of DA cell processes, TH-positive but GFP-negative, coincided with the arborizations, TH-negative but GFP-positive, of the type 2 CA cell dendrites (Fig. 2D). Radial measurements across the IPL of the intensity of the red and green pixel fluorescence confirmed that the vitreal plexus of DA cell processes was in the stratum S3 of the IPL (Fig. 3).

Because of the density of the DA cell plexus in S1, TH immunocytochemistry did not permit us to identify unequivocally the site of origin of the S3 processes from their parent neuron. We therefore penetrated with sharp electrodes the perikarya of DA cells in a superfused retina preparation and iontophoretically injected neurobiotin. DA cell bodies were identified on account of their shape, larger size and weak GFP fluorescence. The retina was subsequently treated with fluorochrome-conjugated streptavidin and DA cells were reconstructed from confocal Z series. In the cell illustrated in Figure 4A, dendrites and axons radiate in all directions from the perikaryon, occasionally crossing each other. The vast majority of processes were confined to the S1 stratum of the IPL. One process, however, marked by the arrowhead in 4A and blue in Figure 4B, descended into the IPL, bent at a right angle and came to lie in S3, as demonstrated by the inset of Figure 4B, in which depth is coded in pseudocolor by the Zeiss LSM software.

These processes in S3 seemed a candidate for the ON bipolar input onto the DA cells. We therefore sought direct evidence for such input by using two independent techniques: the first took advantage of the expression of PLAP by the DA cells, which allowed inspection by electron microscopy. The second relied instead on simple immunostaining, taking advantage of their strong expression of TH: we immunolabeled the DA cell processes in S3 with antibodies against TH and then looked, in triple-labeled material, for evidence of the pre- and postsynaptic specializations of the bipolar cell synapses.

Synaptic Connections of the S3 Processes of DA cells

For demonstration of PLAP enzymatic activity at the light and electron microscopic level, we used a technique based on the hydrolysis of glycerophosphate in the presence of alkaline lead citrate to produce an electron-dense precipitate of lead phosphate (Gustincich et al. 1997). Because PLAP is situated on the outer surface of the cell membrane, the DA cell perikarya and their processes are surrounded in electron micrographs by an amorphous, dense precipitate of lead phosphate that is rigorously confined to the intercellular cleft and does not penetrate the bilayer of the cell membrane or invade the underlying cytoplasm. Thus, synaptic contacts established or received by the labeled processes are readily identified. This enzymatic reaction had the advantage, with respect to electron microscope immunocytochemistry, that the tissue is optimally preserved, but it had the shortcoming that the phosphate ions released by the hydrolysis of glycerophosphate diffused short distances along the intercellular spaces from the PLAP-carrying processes before being captured by the lead ions. This limited diffusion, however, does not interfere significantly with the identification of the processes at the electron microscope as long as the incubation time in the substrate is short.

The technique used to visualize PLAP enzymaticactivity is relatively insensitive. This was to our advantage, because type 2 CA cell bodies and their processes, remained unstained in retinas that were incubated for less than 24 hr in the substrate of the PLAP histochemical reaction. We verified this at the light microscope by converting the lead phosphate reaction product into a precipitate of lead sulfide in 1 μm thick sections of plastic-embedded retinas that had been incubated for 24 hr (Fig. 5). Indeed, the PLAP-positive processes in S3 were distributed at considerable distances from one another rather than forming a continuous plexus as was the case for the GFP-positive dendrites of type 2 CA cells. The distribution of the PLAP-positive processes was therefore consistent with that expected in radial sections through the S3 plexus of TH-positive DA cell processes, such as that illustrated in Figure 2B.

We examined with the electron microscope retinas incubated for 8 hr in the substrate of the PLAP histochemical reaction to minimize diffusion of the reaction product. In the middle of the IPL, synaptic endings were found that established ribbon synapses onto a postsynaptic dyad in which one or both postsynaptic processes were heavily labeled by a dense precipitate of lead phosphate in the surrounding intercellular cleft and therefore belonged to a DA cell (Fig. 6). On the other hand, the presence of a ribbon surrounded by synaptic vesicles and the unique anatomy of the dyad synapse unequivocally identified the presynaptic ending as belonging to a bipolar cell. In places, a labeled postsynaptic process returned a reciprocal synapse onto the bipolar ending (Fig. 6, inset). These bipolar synapses were situated in S3, because they were equidistant from the scleral and vitreal borders of the IPL.

Identification of the Bipolar Synapses by Confocal Microscopy

As expected from the sparseness of the TH-positive plexus in S3 as seen with the light microscope, bipolar-to-DA cell synapses appeared far apart from each other in the electron micrographs. As an independent verification of their existence (and a coarse estimate of their frequency), we used confocal microscopy of tangential cryostat sections of the retina triple-stained for kinesin Kif3a, glutamate receptor subunits and TH. The monoclonal antibody to kinesin Kif3a stained the synaptic ribbons (Muresan et al. 1999; Jeon et al. 2002; Jakobs et al. 2008); the rabbit polyclonals to the AMPA receptor subunits 1 or 2/3 stained the postsynaptic active zone and a sheep polyclonal to TH identified the DA cell processes (Fig. 7A, enlarged in B). Correspondence of the three labels was strikingly frequent: in the field of Figure 7A, a total of ten triple co-localizations are readily observed (arrowheads). If

the same density of puncta – red, green, and blue – in that field are assigned positions at random, the number of triple colocalizations, defined as the three puncta lying within 0.5 μm of each other, is essentially zero (data not shown). Although the necessary thresholding of the puncta adds a level of uncertainty as to their absolute densities, various thresholding criteria did not change the fundamental result.

The spatial density of synapses seen by confocal microscopy could be roughly compared with those seen by electron microscopy. Their density was larger but within the same order of magnitude as that of the varicosities present along the length of the S3 processes in confocal Z series of retinal whole mounts. Occasionally, multiple ribbon synapses were strung out in a row, possibly representing sections of a single DA cell process weaving in and out of the cutting plane.

Since DA cells are also GABAergic (Contini and Raviola 2003; Hirasawa et al. 2009) and, as shown by electron microscopy, their processes in S3 established reciprocal synapses onto the presynaptic bipolars, we also triple-stained retinal sections with antibodies to TH, kinesin Kif3a and both the ⟨1 and β1 subunits of the $GABA_A$ receptor. Again, we observed unique combinations of a ribbon, a receptor patch and a DA cell process that corresponded to the reciprocal DA cell-to-bipolar cell synapses (Fig. 7C).

Correspondence between Light and Electron Microscopy: the Spatial Arrangement of the Pre- and Postsynaptic Active Zones

From the geometry of bipolars' ribbon synapses in electron micrographs, one can predict the appearance at the light microscope of an orthogonal projection of the bipolar-to-DA cell synapse in S3. This correspondence is illustrated in Figure 8: in the electron micrograph of Figure 6, from a radial section of the retina, the DA cell process is colored blue, the ribbon in the adjacent bipolar ending is colored green and the postsynaptic membrane, that contains the ionotropic glutamate receptors, is colored red. Above is shown schematically (colored circles) the orthogonal projection of this synapse as viewed from the vantage point of an observer who looks vertically down onto the synapse (as in the whole-mount view). This exercise provides another check on the veracity of our identification of these contacts with the confocal microscope and provides a key for interpreting oblique projections such as those illustrated in Figure 7.

Discussion

It has been know for a long time that DA cells give rise to processes that course in the middle of the IPL; in the past, however, a search of the bipolar synapses onto those processes was complicated by the presence at the same tangential level of the arborizations of type 2 CA cells, which in many retinas are stained by antibodies to TH. Little is known about this amacrine cell type: they express GFP or PLAP under control of promoter sequences of the gene for TH, but their transmitter is not a conventional catecholamine. Our strategy was to exploit the fact that in both lines of transgenic mice used in this study type 2 CA cells did not stain with antibodies to TH, a property of the C57BL/6J strain of mice and their hybrids. Secondly, because of vagaries in the expression of transgenes containing truncated promoter sequences of different lengths, type 2 CA cells were more intensely fluorescent than DA cells in the GFP mice whereas the reverse was true for transgene expression in the PLAP line. Thus, on the one hand, after staining for TH we could pinpoint the localization of the vitreal processes of DA cells in S3 by their co-stratification with the dendritic arbor of type 2 CA cells. On the other hand, by shortening the incubation time in the histochemical reaction for alkaline phosphatase activity, we could exclusively label the S3 processes of DA cells for the electron microscope.

We could thus establish that the DA cell processes in S3 are postsynaptic to the endings of bipolar cells and, in turn, make reciprocal, conventional synapses onto the presynaptic bipolar. This reciprocal synapse is probably GABAergic, for DA cells release GABA (Hirasawa et al. 2009) and establish GABAergic synapses onto AII amacrine cells, the postsynaptic target of their axons in S1 (Contini and Raviola 2003). Furthermore, because of the unusual geometry of the dyad synapse, by staining simultaneously the synaptic ribbon, the DA cell processes and the postsynaptic patch of ionotropic receptors, we could confirm with the confocal microscope that the bipolar-to-DA cell synapse is glutamatergic and show that the reciprocal, DA cell-to-bipolar synapse is GABAergic. As a general rule, varicosities of neuronal processes are caused by the accumulation of synaptic vesicles and mitochondria at the presynaptic active zone. It is therefore likely that each varicosity along the TH-positive S3 processes of DA cells corresponds to the site of both the excitatory bipolar synapse and the reciprocal, inhibitory DA cell synapse. On account of their synaptology, it is a moot question whether the S3 processes of DA cells are dendrites or axons: in their small diameter and presence of varicosities, they resemble the multiple axons of DA cells in S1, but there is no evidence to date that these axons are also postsynaptic as is the case for the S3 processes.

Since the bipolar cells of the mammalian retina that send their axons to the *b* sublamina of the IPL invariably depolarize upon illumination, we can safely conclude that the dyad synapses in S3 are the site of the elusive ON-bipolar input onto DA cells in the mouse. They are therefore responsible for the increase in dopamine outflow caused by photopic illumination of the intact retina *in vitro* (Kramer 1971; Boatright et al. 1989) and for the light responses recorded from this cell type by Zhang et al. (2007, 2008). The most likely candidate for the bipolar cell type that synapses with DA cells in S3 is the CB3 cone bipolar described in the mouse retina by Pignatelli and Strettoi (2004) or the type 5 cone bipolar in the classification of Ghosh et al. (2004). This is the only bipolar type whose axonal arborizations are confined to S3, where they form an overlapping meshwork twice as dense as that of any other cone bipolar contributing axonal endings to this stratum (Wässle et al. 2009). Although we cannot rule out the possibility that CB3/4 (type 6) bipolars can also be presynaptic to DA cells, they send most of their axonal branches to S4 and S5 (Pignatelli and Strettoi 2004; Wässle et al. 2009).

Hoshi et al. (2009) have recently documented by confocal microscopy the apposition of synaptic ribbons in the axons of calbindin-positive ON bipolar cells with the DA cells processes in stratum S1 of the rabbit IPL, These sites of apposition give every evidence of being *boutons en passant* along the axons of rabbit CBb5 bipolars (MacNeal et al. 2004), as they cross S1 on their way to the boundary between strata S4 and S5. There is no conflict between these results and our own and it seems unlikely that apparent discrepancies are due to species differences: in fact, the mouse also has ectopic bipolar synapses in S1 (Gustincich et al. 1997) and, in the rabbit, DA cells send processes to the ON-sublamina of the IPL (Brecha et al. 1984; Hokoç and Mariani 1988; Tauchi et al. 1990; Casini and Brecha 1992). However, the connectivity of these processes in the rabbit is unknown. The relative importance of the two ON-inputs onto DA cells is unclear: electron microscopy of serial sections will be required to establish whether in the mouse S1 and S3 synapses are established by the same type of bipolar cell, the CB3 mouse bipolar. If this were the case, it would not be surprising that a bipolar axon that ultimately synapses with DA cells in S3, would also connect *en passant* with their dendrites in S1.

In the rabbit, the S1 synapses are established by another type of bipolar cell, the CBb5 variety, which may have a different functional role than the mouse CB3. It is intriguing that the S1 input in the rabbit appears to occur via a specialized type of bouton, termed “giant puncta” by Hoshi et al. (2009). Their morphological distinctiveness suggests a distinct

physiological functional role as well; it remains to be learned. Finally, it must be noted that an input from OFF-cone bipolars cannot yet be ruled out completely, because there is a basal release of dopamine in the dark. This transmitter output, however, is probably sustained by the persistence of their spontaneous activity in absence of illumination (Zhang et al. 2007, 2008).

Recently, it has been suggested that the population of DA cells is physiologically heterogeneous (Zhang et al. 2007,2008): 32 to 40% of these neurons were apparently unresponsive to light, about half of them generated transient light responses mediated by their input from ON-bipolars and, finally, 16 to 21% exhibited sustained responses that persisted after pharmacological block of synaptic transmission from photoreceptors to ON-bipolars. These last responses, on account of their latency, duration and spectral properties were attributed to an input from melanopsin-expressing ganglion cells (Zhang et al. 2008). Because of these observations, the question arises whether all DA cells contribute processes to the TH-positive plexus in S3 and therefore receive synapses from ON-bipolars. Considering that (i) there are only about 600 DA cells in the mouse; (ii) they are uniformly distributed throughout the retina; (iii) they do not fall into three distinct anatomical categories (unpublished observations); and (iv) their S3 processes form a continuous, uniform plexus throughout the retina, our results suggest that each DA cell could conceivably receive 30 to 50 synapses from ON-bipolars. An attempt to clarify this issue by injecting DA cell with neurobiotin was inconclusive: because of the possibility of incomplete filling with the tracer, absence of staining of the S3 processes does not prove that they do not exist. On the other hand, the absence of light responses in a physiological experiment on an isolated retina does not necessarily rule out the presence of bipolar synapses.

In conclusion, this study, combined with previous observations that DA cells release GABA (Hirasawa et al. 2009) and are presynaptic at GABAergic synapses (Contini and Raviola 2003), suggests an attractive hypothesis for the functional connectivity of this cell type: when the retina is illuminated with bright light (i) DA cells are depolarized at the glutamatergic dyad synapses established in S3 by ON-bipolars. (ii) As is the rule for most amacrine cells, they exert an inhibitory feedback onto the presynaptic bipolars. (iii) They release dopamine, which diffuses throughout the retina and, acting by volume transmission, sets the gain of the retinal circuits for cone vision. And finally, (iv) by exerting a powerful GABAergic inhibition on AII amacrine cells, they prevent the noise of the saturated rods from entering the cone pathway.

Supplementary Material

Refer to Web version on PubMed Central for supplementary material.

Acknowledgments

We thank W. Siegart for the antibodies to the α1 and β1 subunit of the $GABA_A$ receptor and Ms. Hong Lu for technical assistance.

Funded by: National Institutes of Health; Grant Numbers: EY01344 and EY017169. RHM is a Senior Investigator of Research to Prevent Blindness.

Literature Cited

Bjelke B, Goldstein M, Tinner B, Andersson C, Sesack SR, Steinbusch HWM, Lew JY, He X, Watson S, Tengroth B, Fuxe K. Dopaminergic transmission in the rat retina: evidence for volume transmission. J Chem Neuroanatomy. 1996; 12:37–50.

Boatright JH, Hoel MJ, Iuvone PM. Stimulation of endogenous dopamine release and metabolism in amphibian retina by light- and K^+-evoked depolarization. Brain Res. 1989; 482:164–168. [PubMed: 2706474]

Brecha NC, Oyster CW, Takahashi ES. Identification and characterization of tyrosine hydroxylase immunoreactive amacrine cells. Invest Ophthalmol Vis Sci. 1984; 25:66–70. [PubMed: 6142028]

Cajal SR. La rétine des vertébrés. La Cellule. 1893; 9:119–257.

Casini G, Brecha NC. Postnatal development of tyrosine hydroxylase immunoreactive amacrine cells in the rabbit retina: I. Morphological characterization. J Comp Neurol. 1992; 326:283–301. [PubMed: 1479076]

Contini M, Raviola E. GABAergic synapses made by a retinal dopaminergic neuron. Proc Nat Acad Sci USA. 2003; 100:1358–1363. [PubMed: 12547914]

Dacey DM. Dopamine-accumulating retinal neurons revealed by in vitro fluorescence display a unique morphology. Science. 1988; 240:1196–1198. [PubMed: 3375811]

Dacey DM. The dopaminergic amacrine cell. J Comp Neurol. 1990; 301:461–489. [PubMed: 1979792]

Djamgoz MB, Wagner HJ. Localization and function of dopamine in the adult vertebrate retina. Neurochem Int. 1992; 20:139–191. [PubMed: 1304857]

Dorenbos R, Contini M, Hirasawa H, Gustincich S, Raviola E. Expression of circadian clock genes in retinal dopaminergic cells. Visual Neurosci. 2007; 24:573–580.

Dowling JE, Ehinger B. Synaptic organization of the amine-containing interplexiform cells of the goldfish and Cebus monkey retinas. Science. 1975; 188:270–273. [PubMed: 804181]

Dowling JE, Ehinger B. Synaptic organization of the dopaminergic neurons in the rabbit retina. J Comp Neurol. 1978; 180:203–220. [PubMed: 207745]

Dowling JE, Ehinger B, Florén I. Fluorescence and electron microscopical observations on the amine-accumulating neurons of the cebus monkey retina. J Comp Neurol. 1980; 192:665–685. [PubMed: 6252252]

Euler T, Schneider H, Wässle H. Glutamate responses of bipolar cells in a slice preparation of the rat retina. J Neurosci. 1996; 16:2934–2944. [PubMed: 8622124]

Famiglietti EV, Kolb H. Structural basis for On- and Off-center responses in retinal ganglion cells. Science. 1976; 194:193–195. [PubMed: 959847]

Frederick JM, Tayborn ME, Laties AM, Lam DMK, Hollyfield JG. Dopaminergic neurons in the human retina. J Comp Neurol. 1982; 210:65–79. [PubMed: 6127354]

Ghosh KK, Bujan S, Haverkamp S, Feigenspan A, Wässle H. Types of bipolar cells in the mouse retina. J Comp Neurol. 2004; 469:70–82. [PubMed: 14689473]

Gustincich S, Feigenspan A, Wu D-K, Koopman LJ, Raviola E. Control of dopamine release in the retina: a transgenic approach to neural networks. Neuron. 1997; 18:723–736. [PubMed: 9182798]

Gustincich S, Feigenspan A, Sieghart W, Raviola E. Composition of $GABA_A$ receptors of retinal dopaminergic neurons. J Neurosci. 1999; 19:7812–7822. [PubMed: 10479684]

Hirasawa H, Puopolo M, Raviola E. Extrasynaptic release of GABA by retinal dopaminergic neurons. J Neurophysiol. 2009; 102:146–158. [PubMed: 19403749]

Hokoç JN, Mariani AP. Tyrosine hydroxylase immunoreactivity in the rhesus monkey retina reveals synapses from bipolar cells to dopaminergic amacrine cells. J Neurosci. 1987; 7:2785–2793. [PubMed: 2887643]

Hokoç JN, Mariani AP. Synapses from bipolar cells onto dopaminergic amacrine cells in cat and rabbit retinas. Brain Res. 1988; 461:17–26. [PubMed: 2906268]

Hoshi H, Liu W-L, Massey SC, Mills SL. ON inputs to the OFF layer: bipolar cells that break the stratification rules of the retina. J Neurosci. 2009; 29:8875–8883. [PubMed: 19605625]

Jakobs TC, Koizumi A, Masland RH. The spatial distribution of glutamatergic inputs to dendrites of retinal ganglion cells. J Comp Neurol. 2008; 510:221–236. [PubMed: 18623177]

Jeon CJ, Kong JH, Strettoi E, Rockhill R, Stasheff SF, Masland RH. Pattern of synaptic excitation and inhibition upon direction-selective retinal ganglion cells. J Comp Neurol. 2002; 449:195–205. [PubMed: 12115689]

Kolb H, Cuenca N, Wang HH, Dekorver L. The synaptic organization of the dopaminergic amacrine cell in the cat retina. J Neurocytol. 1990; 19:343–366. [PubMed: 2391538]

Kramer SG. Dopamine: a retinal neurotransmitter. I. Retinal uptake, storage, and light-stimulated relase of H3-dopamine in vivo. Invest Ophthalmol. 1971; 10:438–452. [PubMed: 4325307]

MacNeal MA, Heussy JK, Dacheux RE, Raviola E, Masland RH. The population of bipolar cells in the rabbit retina. J Comp Neurol. 2004; 472:73–86. [PubMed: 15024753]

Mariani AP, Hokoç JN. Two types of tyrosine hydroxylase-immunoreactive amacrine cell in the rhesus monkey retina. J Comp Neurol. 1988; 276:81–91. [PubMed: 2903868]

Matsushita N, Okada H, Yasoshima Y, Takahashi K, Kiuchi K, Kobayashi K. Dynamics of tyrosine hydroxylase promoter activity during midbrain dopaminergic neuron development. J Neurochem. 2002; 82:295–304. [PubMed: 12124430]

Mayahara H, Hirano H, Saito T, Ogawa K. The new lead citrate method for the ultracytochemical demonstration of activity of non-specific alkaline phosphatase (orthophosphoric monoester phosphohydrolase). Histochemie. 1967; 11:88–96. [PubMed: 5589645]

McGillem GS, Dacheux RF. Rabbit cone bipolar cells: correlation of their morphologies with whole-cell recordings. Vis Neurosci. 2001; 18:675–685. [PubMed: 11925003]

Muresan V, Lyass A, Schnapp BJ. The kinesin motor Kif3a is a component of the presynaptic ribbon in vertebrate photoreceptors. J Neurosci. 1999; 19:1027–1037. [PubMed: 9920666]

Nelson R, Famiglietti EV, Kolb H. Intracellular staining reveals different levels of stratification for ON- and OFF-center ganglion cells in cat retina. J Neurophys. 1978; 41:472–483.

Nguyen-Legros J. Morphology and distribution of catecholamine-neurons in mammalian retina. Progr Retinal Res. 1988; 7:113–147.

Nguyen-Legros J, Berger B, Vigny A, Alvarez C. Tyrosine hydroxylase-like immunoreactive interplexiform cells in the rat retina. Neurosci Lett. 1981; 27:255–259. [PubMed: 6120490]

Nguyen-Legros J, Berger B, Vigny A, Alvarez C. Presence of interplexiform dopaminergic neurons in the rat retina. Brain Res Bull. 1982; 9:379–381. [PubMed: 6129041]

Nusser Z, Roberts JDB, Baude A, Richards JG, Sieghart W, Somogyi P. Immunocytochemical localization of the α1 and β2/3 subunits of the $GABA_A$ receptor in relation to specific GABAergic synapses in the dentate gyrus. Eur J Neurosci. 1995; 7:630–646. [PubMed: 7620614]

Pignatelli V, Strettoi E. Bipolar cell of the mouse retina: A gene gun, morphological study. J Comp Neurol. 2004; 476:254–266. [PubMed: 15269969]

Pourcho RG. Dopaminergic amacrine cells in the cat retina. Brain Res. 1982; 252:101–109. [PubMed: 7172014]

Puopolo M, Hochstetler SE, Gustincich S, Wightman RM, Raviola E. Extrasynaptic Release of Dopamine in a Retinal Neuron: Activity Dependence and Transmitter Modulation. Neuron. 2001; 30:211–225. [PubMed: 11343656]

Sperk G, Schwarzer C, Tsunashima K, Fuchs K, Sieghart W. $GABA_A$ receptor subunits in the rat hippocampus I: Immunocytochemical distribution of 13 subunits. Neuroscience. 1997; 80:987–1000. [PubMed: 9284055]

Tauchi M, Madigan NK, Masland RH. Shapes and distributions of the catecholamine-accumulating neurons in the rabbit retina. J Comp Neurol. 1990; 293:178–189. [PubMed: 19189710]

Törk I, Stone J. Morphology of catecholamine-containing amacrine cells in the cat's retina, as seen in retinal whole mounts. Brain Res. 1979; 169:261–273. [PubMed: 445157]

Voigt T, Wässle H. Dopaminergic innervation of AII amacrine cells in mammalian retina. J Neurosci. 1987; 7:4115–4128. [PubMed: 2891802]

Wang HH, Cuenca N, Kolb H. Development of morphological types and distribution patterns of amacrine cells immunoreactive to tyrosine hydroxylase in the cat retina. Vis Neurosci. 1990; 4:159–175. [PubMed: 1980203]

Wässle H, Puller C, Müller F, Haverkamp S. Cone contacts, mosaics, and territories of bipolar cells in the mouse retina. J Neurosci. 2009; 29:106–117. [PubMed: 19129389]

Witkovsky P. Dopamine and retinal function. Documenta Ophthalmologica. 2004; 108:17–40. [PubMed: 15104164]

Witkovsky P, Dearry A. Functional roles of dopamine in the vertebrate retina. Progr Retinal Res. 1991; 11:247–292.

Witkovsky P, Arango-Gonzalez B, Haycock JW, Kohler K. Rat retinal dopaminergic neurons: differential maturation of somatodendritic and axonal compartments. J Comp Neurol. 2005; 481:352–362. [PubMed: 15593337]

Witkovsky P, Nicholson C, Rice ME, Bohmaker K, Meller E. Extracellular dopamine concentration in the retina of the clawed frog, *Xenopus laevis*. Proc Natl Acad Sci USA. 1993; 90:5667–5671. [PubMed: 8516316]

Witkovsky P, Veisenberger E, LeSauter J, Yan L, Johnson M, Zhang DQ, McMahon D, Silver R. Cellular location and circadian rhythm of expression of the biological clock gene Period 1 in the mouse retina. J Neurosci. 2003; 23:7670–7676. [PubMed: 12930806]

Wulle I, Schnitzer J. Distribution and morphology of tyrosine hydroxylase-immunoreactive neurons in the developing mouse retina. Brain Res Dev Brain Res. 1989; 48:59–72.

Zezula J, Sieghart W. Isolation of type I and type II $GABA_A$-benzodiazepine receptors by immunoaffinity chromatography. Fedn Eur Biochem Socs Lett. 1991a; 284:15–18.

Zezula J, Fuchs K, Sieghart W. Separation of α_1-, α_2- and α_3- subunits of the $GABA_A$ benzodiazepine receptor complex by immunoaffinity chromatography. Brain Res. 1991b; 563:325–328. [PubMed: 1664775]

Zhang D-Q, Wong KY, Sollars PJ, Berson DM, Pickard GE, McMahon DG. Intraretinal signaling by ganglion cell photoreceptors to dopaminergic amacrine neurons. Proc Nat Acad Sci USA. 2008; 105:14181–14186. [PubMed: 18779590]

Zhang D-Q, Zhou T-R, McMahon DG. Functional heterogeneity of retinal dopaminergic neurons underlying their multiple roles in vision. J Neurosci. 2007; 27:692–699. [PubMed: 17234601]

Zimprich F, Zezula J, Sieghart W, Lassmann H. Immunohistochemical localization of the α_1-, α_2- und α_3- subunit of the $GABA_A$ receptor in the rat brain. Neurosci Lett. 1991; 127:125–128. [PubMed: 1715535]

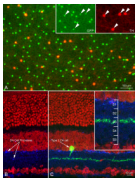

Figure 1.

(A) Confocal image of the inner nuclear layer of a retinal whole mount from a transgenic mouse in which both DA cells and type 2 CA cells express GFP (green) under control of a TH promoter sequence. The retina was stained with antibodies to TH (red). Only DA cell perikarya are positive to TH (**Inset**); furthermore, in DA cells GFP fluorescence is weaker and largely confined to the nucleus. Figure 1A is available as a magenta-green supplementary copy. **(B)** In this radial section of the retina of a mouse belonging to the same transgenic line as in A, DA cell processes are stained blue by an antibody to TH and the nuclei are stained red by ethidium bromide. The green channel was omitted to show that the processes of type 2 CA cells are not stained by TH antibodies. **(C)** Same specimen as in B. Type 2 CA cells show intense GFP fluorescence. Their small perikaryon gives rise to a single apical dendrite that descends vertically to the middle of the IPL and resolves into a dense plexus, rigorously confined to the center of the S3 stratum (**Inset**). Figure 1A is available as a magenta-green supplementary copy.

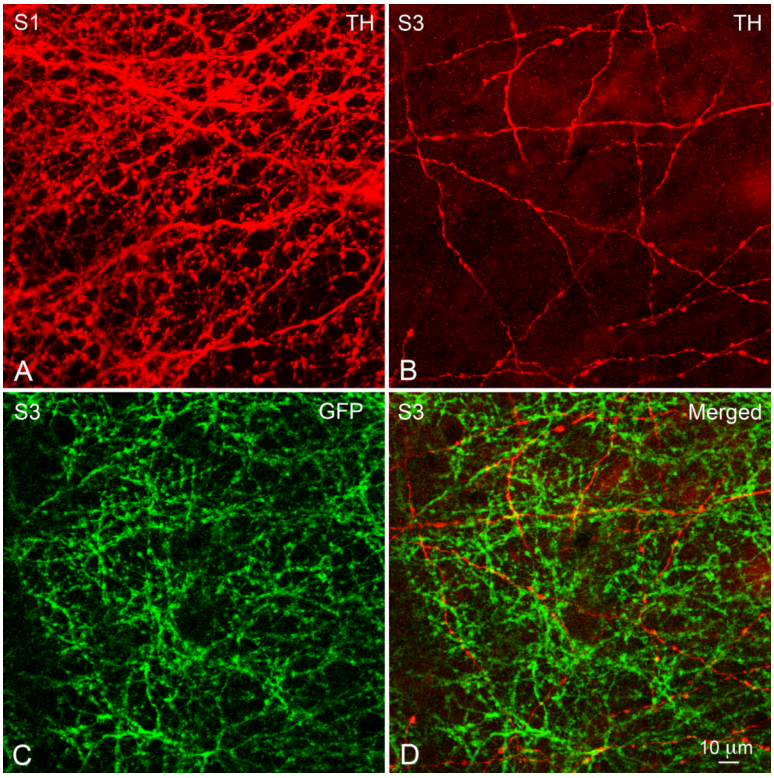

Figure 2.

Micrographs from a confocal Z series of the IPL in a whole mount of the retina processed as in Figure 1A. **(A)** The TH-positive processes emanating from the body of DA cells form an inextricable plexus in the S1 stratum of the IPL, perforated by circular openings occupied by the perikarya of AII amacrine cells. **(B)** From the S1 plexus descending processes traverse the scleral half of the IPL and finally run a long, tangential course in the stratum S3. Here, they cross each other at various angles, forming a loose plexus that delimits wide, irregular meshes. Note the varicosities occurring at irregular intervals along the length of the processes. **(C)** The dendritic arbors of type 2 CA cells, which exhibit intense GFP fluorescence but are TH-negative, form a dense network in S3 that coincides with the sparse plexus of the TH-positive but GFP-negative processes of DA cells **(D)**. This figure is available as a magenta-green supplementary copy.

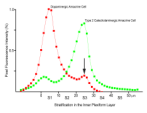

Figure 3.

The intensity of the red (TH) and green (GFP) fluorescence was measured in 50 consecutive, 1 μm-thick, tangential optical sections of the confocal Z series through the IPL illustrated in Figure 2. The resulting diagram confirms that the vitreal plexus of DA cell processes (arrow) coincides with the dendritic arborizations of type 2 CA cells in the stratum S3 of the IPL. This figure is available as a magenta-green supplementary copy.

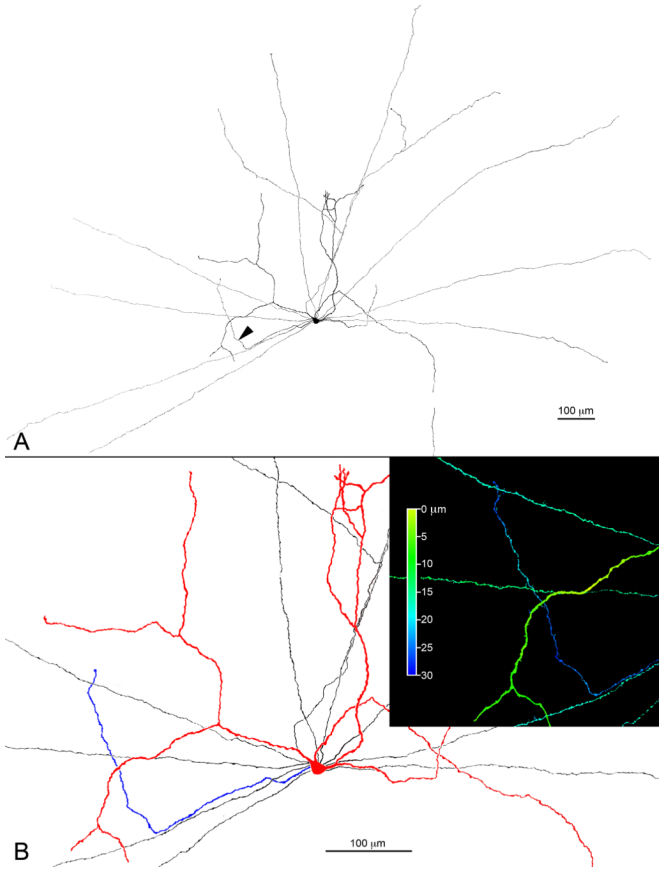

Figure 4.

(A) Orthogonal projection of a DA cell that was injected with neurobiotin, stained with fluorochrome-conjugated streptavidin and reconstructed from a mosaic of confocal Z-series. The cell has dendrites (colored red in Fig. 4B) and axons (black in Fig. 4B), all confined to the S1 stratum of the IPL. One process, however, colored blue in Figure 4B, descends into the IPL, bends at a right angle and comes to lie in S3, as demonstrated by the **inset** in which depth in the IPL is coded in pseudocolor by the Zeiss confocal LSM software. This figure is available as a magenta-green supplementary copy.

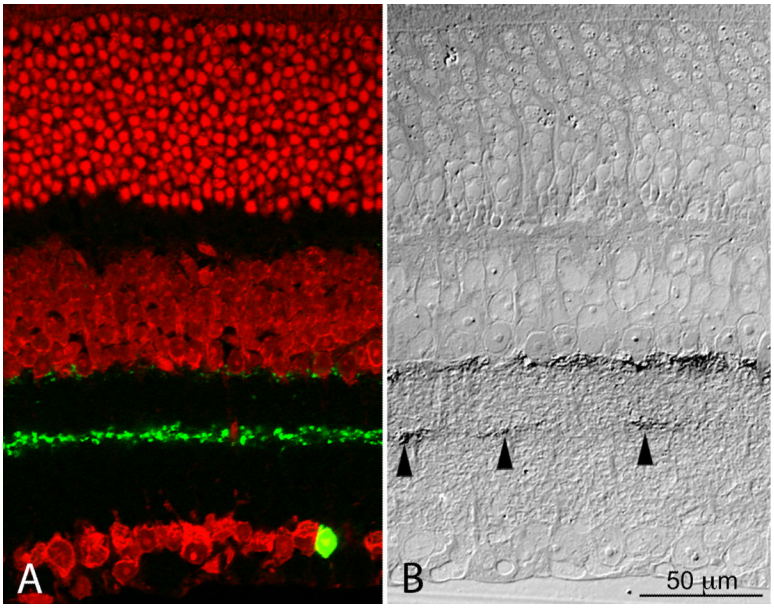

Figure 5.

Side by side light micrographs of a cryostat section of the retina of a GFP mouse (**A**) and a section of a plastic-embedded retina in which DA cells express PLAP under control of a TH promoter sequence (**B**). In the stratum S3 of the IPL the GFP-positive dendrites of type 2 CA cells **(A)** form a dense, continuous plexus. In contrast, the PLAP-positive processes (**B**, arrowheads) are much fewer in number and scattered at a considerable distance from one another. **A)** Confocal image after staining of the nuclei with ethidium bromide. **B)** DIC micrograph of a 1 µm section of a retina incubated for 24 hr in the substrate for alkaline phosphatase histochemistry. The lead phosphate reaction product was converted into lead sulfide, which is visible with the light microscope. The size of the PLAP-positive spots is larger than the diameter of the DA cell processes in S3 because of the diffusion of the reaction product with the long incubation time. Because of the shrinkage of the retina with dehydration and embedding, the micrograph on the right was enlarged until the distance between inner and outer limiting membranes coincided with that of the retinal section on the left. This figure is available as a magenta-green supplementary copy.

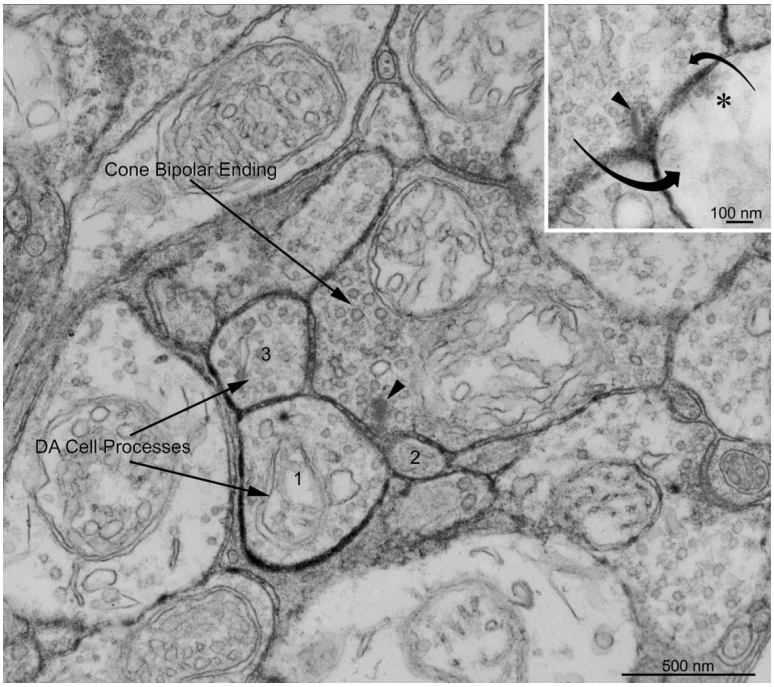

Figure 6.

Electron micrograph of the retina of a PLAP mouse stained with the histochemical reaction for demonstration of PLAP enzymatic activity. The incubation time (8 hr) was shorter than in Figure 5B to minimize diffusion of the reaction product. An axonal ending of a bipolar cell, identified because of the presence of a synaptic ribbon (arrowhead), establishes a dyad synapse onto a pair of postsynaptic processes of which one (1) is heavily labeled by a dense precipitate of lead phosphate in the surrounding intercellular cleft and therefore belongs to a DA cell. The other, smaller member of the postsynaptic dyad (2) is weakly labeled, possibly by reaction product diffusing from the cleft surrounding the heavily labeled partner. A second DA cell process (3) receives synaptic input from the same bipolar ending out of the plane of section, as evidenced by the enlargement of the intervening cleft and the presence of pre- and postsynaptic densities. The bipolar ending is situated in S3 because it is equidistant from the scleral and vitreal borders of the IPL. **Inset:** a labeled postsynaptic process returns a reciprocal synapse onto the bipolar ending: the arrows indicate the direction of the synaptic influences. The bipolar ribbon is indicated by an arrowhead and the active zone of the reciprocal synapse is marked by an asterisk.

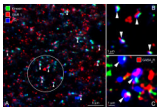

Figure 7.

(A) In a tangential cryostat section through the S3 stratum of the IPL, several bipolar-to-DA cell ribbon synapses (arrowheads) can be identified with the confocal microscope, based on the topographic association of a synaptic ribbon (stained green by an antibody to kinesin Kif3a), an aggregate of AMPA receptors (stained red by an antibody to the GluR1 subunit) and the cytoplasm of a DA cell process (stained blue by an antibody to TH). **(B)** Higher magnification of four ribbon synapses contained in Figure 7A (circle). **(C)** Three instances of topographic association of a ribbon (green) with an aggregate of ⟨1 and ® 1 subunits of the $GABA_A$ receptor (red, $GABA_A$ R) and a DA cell process (blue). These images probably correspond to GABAergic reciprocal synapses established by DA cell processes onto the presynaptic bipolar ending.

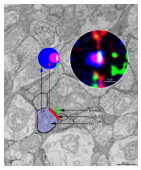

Figure 8.
Diagram illustrating the appearance of an orthogonal projection of a bipolar-to-DA cell ribbon synapse in a retinal cryostat section triple-stained with antibodies to kinesin Kif3a (green), AMPA glutamate receptor subunits GluR 2/3 (red) and TH (blue). The postsynaptic aggregate of glutamate receptors, stained red, appears purple when superimposed on the DA cell process, that is stained blue. In turn, the synaptic ribbon appears white when superimposed on the purple of the receptor cluster and aqua when overlapping the blue cytoplasm of the DA cell process. Probably the aqua portion of the ribbon overhangs the other member of the postsynaptic dyad.

Table 1

Antigen	Immunogen	Manufacturer, type of antibody, catalog number	Dilution
Tyrosine hydroxylase[1]	Tyrosine hydroxylase purified from PC12 cells	Immunostar Inc., Hudson, WI, mouse monoclonal, Cat. #22941	1: 500
Tyrosine hydroxylase[2]	Tyrosine hydroxylase purified from rat pheochromocytoma	Novus Biologicals, Littleton, CO, sheep polyclonal, Cat. #NB 300-110	1: 500
Kinesin II[3]	Sea urchin egg cytosol	Covance, Emeryville, CA mouse monoclonal, Cat#MAB1613	2-4 μg/ml
glutamate receptor 1[4]	Carboxy terminus peptide of rat GluR1 (SHSSGMPLGATGL) conjugated to BSA with glutaraldehyde	Chemicon (Millipore, Billerica, MA), rabbit polyclonal, Cat. #AB1504	1-3 μg/ml
glutamate receptors[5] 2/3	Carboxy terminus peptide of rat GluR2 (EGYNVYGIESVKI) conjugated to BSA with glutaraldehyde	Chemicon (Millipore, Billerica, MA), rabbit polyclonal, Cat. #AB1506	1-3 μg/ml
⟨1 subunit of the $GABA_A$ receptor[6]	Synthetic peptide, aa 1-9 from rat N-terminus, coupled to keyhole-limpet haemocyanin	gift from W. Sieghart, rabbit polyclonal	1.8 μg/ml
®1 subunits of the $GABA_A$ receptor[7]	Recombinant fusion protein containing aa 350-404 from rat N-terminus	gift from W. Sieghart, rabbit polyclonal	1.8 μg/ml